

Discrete Trigonometric Transform Thermography for Defect Detection in Composites

by I. Lasso-Martinez*, H. Loaiza-Correa* and A. Restrepo-Giron*

* Universidad del Valle, Programa de Posgrados en Ingeniería Eléctrica y Electrónica, Cali, Colombia, {ivan.lasso, humberto.loaiza, andres.david.restrepo} @correounivalle.edu.co

Abstract

Images obtained with Pulsed Thermography (PT) are often affected by noise and non-uniform heating. Therefore, numerous advanced signal processing methods have been proposed to solve these problems and thus improve the defects detection that are below the surface of materials. Some of these techniques are Principal Component Thermography (PCT), High-Order Statistics (HOS), Thermographic Signal Reconstruction (TSR) –and its first and second derivatives–. However, none of these methods is based on the law of conservation of energy of a signal (i.e., each image or thermogram) between space and frequency domains. With this approach we developed an algorithm to detect defects in Carbon Fiber Reinforced Plastic (CFRP) composites. To do this we evaluated four types of Discrete Cosine Transforms (DCTs): DCT-1, DCT-2, DCT-3, DCT-4; and four types of Discrete Sine Transforms (DSTs): DST-1, DST-2, DST-3, DST-4. Comparison between results of the Contrast-to-Noise Ratio (CNR) metric shows that if the proposed algorithm uses DCT-1, then it outperforms second derivative of the TSR. Furthermore, this method is robust to noise and changes in the center and shape of non-uniform heating. After an extensive literature search, no reports on the use of these transforms in pulsed thermography were found.

1. Introduction

The DCTs/DSTs began to be discovered by the electronic engineer Nasir Ahmed in 1974. In total there are sixteen transforms, eight DCT and eight DST. The most popular is the DCT-2 for its property of compacting the energy in very few coefficients of the image spectrum. Two of the direct two-dimensional definitions of the DCTs/DSTs tested are presented in Eqs. (1) and (2).

$$\text{DCT-1: } X^{c1}(k_1, k_2) = p(k_1)p(k_2) \sum_{n_1=0}^{N_1-1} \sum_{n_2=0}^{N_2-1} q(n_1)q(n_2)x(n_1, n_2) \cos\left(\frac{2\pi}{2(N_1-1)}n_1k_1\right) \cos\left(\frac{2\pi}{2(N_2-1)}n_2k_2\right) \quad (1)$$

$$\text{DCT-2: } X^{c2}(k_1, k_2) = p(k_1)p(k_2) \sum_{n_1=0}^{N_1-1} \sum_{n_2=0}^{N_2-1} x(n_1, n_2) \cos\left(\frac{\pi}{2N_1}(2n_1+1)k_1\right) \cos\left(\frac{\pi}{2N_2}(2n_2+1)k_2\right) \quad (2)$$

where,

- $x(n_1, n_2)$ is each image coming from the thermal camera (i.e., the thermograms).
- N_1, N_2 are the number of rows and columns of each thermogram.
- n_1, n_2 are the pixel coordinates (in the spatial domain) of the thermogram $x(n_1, n_2)$.
- k_1, k_2 are the coefficient coordinates (in the frequency domain) of the transformed thermogram $X(k_1, k_2)$.
- $X^{c1}(k_1, k_2)$ is the transformed thermogram obtained by applying DCT-1 to $x(n_1, n_2)$.
- $X^{c2}(k_1, k_2)$ is the transformed thermogram obtained by applying DCT-2 to $x(n_1, n_2)$.
- $p(k_1), p(k_2), q(n_1), q(n_2)$ are weighting functions to ensure energy conservation between the spatial domain and the frequency domain.

To calculate the DCT/DST to a thermogram ($N_1 \times N_2$ matrix), simply calculate the one-dimensional transform to each row and each column of that thermogram. This can be done since the DCTs/DSTs have separable basis functions.

2. Materials and Methods

As materials, Infrared image sequences obtained with an experimental set-up consisting of a FLIR X8501sc camera, electric charge and synchronization units, and two Balcar FX60 flashes were used. The tested specimen was a flat CFRP sheet with 25 Teflon inlays inside to mimic defects. The defects are found at depths of 0.2 mm, 0.4 mm, 0.6 mm, 0.8 mm and 1.0 mm; and have sizes of 3 x 3 mm², 5 x 5 mm², 7 x 7 mm², 10 x 10 mm² and 15 x 15 mm².

Regarding the methods, the main procedure of this algorithm consists of taking each thermogram of the infrared image sequence and transforming it with each of the DCTs/DSTs. Then, in the frequency domain, those coefficients that store the energy associated with non-uniform heating are eliminated. Such coefficients are concentrated in the lowest values of k_1 and k_2 , next to the origin of coordinates. Subsequently, the thermogram is returned to the spatial domain with the corresponding inverse transform.



3. Results and Conclusion

The most remarkable result was to make an association between the non-uniform heating and the coefficients of the image spectrum, which allows to eliminate these coefficients and consequently eliminate the non-uniform heating regardless of its shape or the location of its center. This is very convenient in case there are changes in the orientation of the heat sources (i.e. the flashes). Figure 1 shows as an example thermogram 13 –from infrared inspection of CFRP– before and after processing with DCT-1.

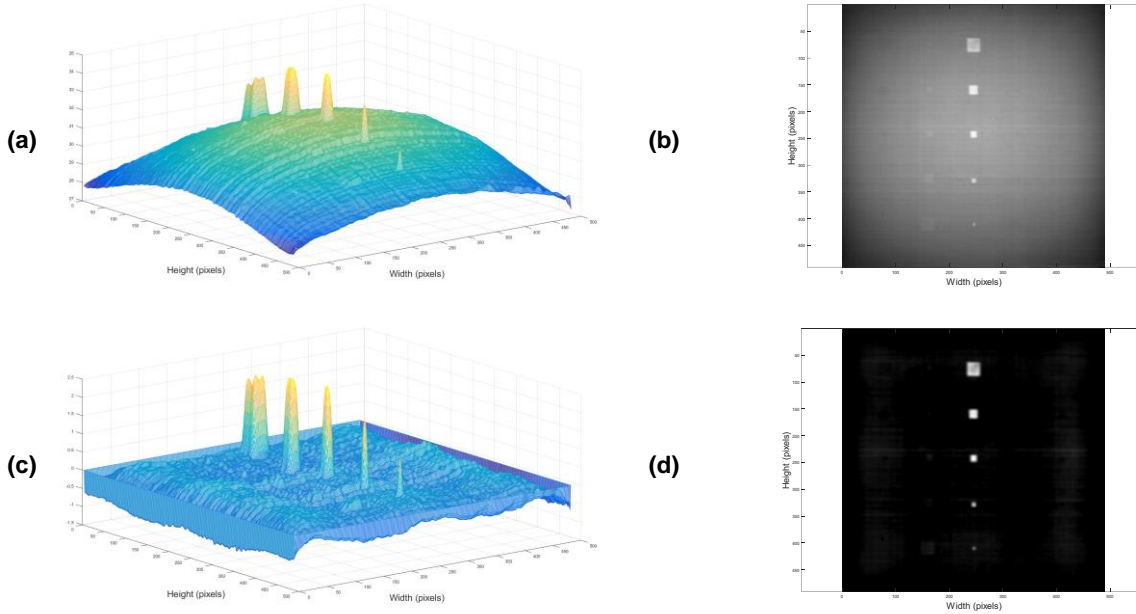


Fig. 1. Thermogram 13 of the infrared inspection. The central column of defects located at a 0.2 mm depth in the CFRP plate is observed. (a) and (b) before processing it with DCT-1. (c) and (d) after processing it with DCT-1.

Figure 2 shows CNR plots of the five largest defects, size 15 x 15 mm². The CNR was measured for each defect in all thermograms, which were processed with the proposed method based on DCT-1 and compared with the second derivative of the TSR. Figure 3(a) shows that in all measures of maximum CNR, DCT-1 outperforms TSR 2nd derivative.

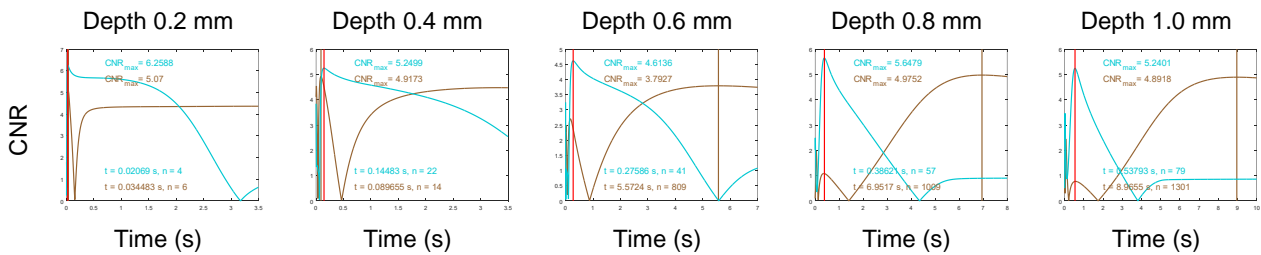


Fig. 2. CNR for second derivative of the TSR (brown plots) and DCT-1 (aquamarine plots). The vertical lines indicate the maximum CNR and its time. All plots for the same infrared inspection. Size of defects: 15 x 15 mm²

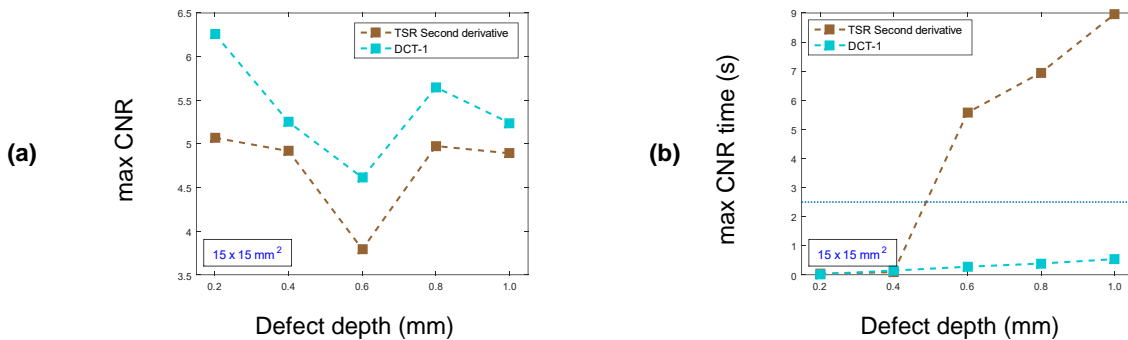


Fig. 3. Comparisons between second derivative of the TSR and DCT-1. Size of defects: 15 x 15 mm². (a) maximum CNR as a function of the defect depth. (b) maximum CNR time as a function of the defect depth.